Materials Transactions, Vol. 43, No. 8 (2002) pp. 1873 to 1878
Special Issue on Lead-Free Electronics Packaging

Thermodynamics-Aided Alloy Design and Evaluation of Pb-free Solders for High-Temperature Applications

Jong Hoon Kim, Sang Won Jeong and Hyuck Mo Lee *

Department of Materials Science and Engineering, Korea Advanced Institute of Science and Technology, Kusung-Dong 373-1, Yusung-Gu Taejon 305-701, Korea

High temperature solders that will not be affected in the subsequent thermal treatment are required in the step soldering process of multi-chip module (MCM) packaging. High-Pb solder alloys such as 95Pb–5Sn (numbers are all in mass% unless specified otherwise) are currently being used for this purpose. However, the development of the Pb-free solder alloy for high temperature applications is needed due to environmental issues. The solder alloys of Bi–Ag, Sn–Sb and Au–Sb–Sn systems are considered as candidates in this study. Aided by thermodynamic calculations, several specific compositions have been chosen and they were investigated in terms of melting behavior, electrical resistivity, wetting angle and hardness. The Bi–Ag alloy exhibited poor electro-conductivity while the Sn–Sb system had low melting temperatures. The ternary Au–Sn–Sb solder alloy shows prospects for high temperature applications in spite of poor wetting properties.

(Received March 15, 2002; Accepted May 21, 2002)

Keywords: *alloy design, lead-free solder, high-temperature solder, step soldering, tin–antimony, bismuth–silver, gold–tin–antimony*

1. Introduction

Advanced packaging technology is required because electronic devices are operating faster and becoming smaller, lighter and more functional. As a result, many advanced packaging technologies such as flip-chip technology, ball grid array (BGA), chip-scale package (CSP) and multi-chip module (MCM) have been developed. The MCM, one of the most advanced forms of electronic packaging, is a group of highly functional electronic devices interconnected to the substrate by fine-line circuitry, usually in the form of multilayers. The significant benefit of MCM is the increased system performance that results from the drastically shortened interconnection length between integrated circuit devices (chips).[1)] When integrated circuit chips are packaged in MCM, step soldering is used. Step soldering is a method to solder various levels of the package with different solders of different melting points so that the soldering of each successive level or step does not melt the previously soldered joint inadvertently.[2)] In general, the 95Pb–5Sn solder with a melting temperature of 308–312°C is used for high temperature applications in step soldering. However, due to environmental issues, the use of Pb is restricted and new Pb-free high temperature solder alloys are required.

In designing new Pb-free high temperature solder alloys, the melting behavior is important. In recent MCM packages, polymers are used as dielectric materials in the substrate, which implies that the glass transition temperature of the polymer, around 350°C,[3)] may be the upper limit of temperature in soldering. The subsequent process temperature is the lower limit of melting points of solders so that the soldered joints should not melt in the subsequent process. Pb-free solder alloys that satisfy this melting characteristic are necessary. The mechanical and electrical properties of solders are important, too, because solder joints connect mechanically and electrically integrated circuit chips with the substrate.

In this study, the Sn–Sb, Bi–Ag and Au–Sn–Sb alloys were selected to replace 95Pb–5Sn for step soldering used in MCM and they were investigated in terms of melting behavior, electrical resistivity, wettability and hardness. Solder alloys with optimum properties will be determined in this way.

2. Experimental Procedures

All alloys were prepared from pure metals (purity higher than 99.9%). Samples were encapsulated in quartz tubes under vacuum, melted and mechanically mixed. As-cast alloys were obtained by cooling in air. X-ray diffraction (XRD) measurements were performed to identify the phases formed in the solder alloys, and energy-dispersive X-ray (EDX) analyses were used to measure compositions. The microstructures were observed using scanning electron microscopy (SEM).

Vickers hardness tests were performed at a load of 300 g in order to examine the mechanical properties. The electrical resistivity was measured from thin foil samples. The 50 to 150 μm thin foil samples were prepared by melting a small amount of solder placed between two sheets of plate glass in a nitrogen-purged oven at 350°C.[4)] The electrical resistivity was measured by four-point probe. To check the current method, pure Sn and Bi foils were prepared in the same way and their resistivity measured 11.77 and 107 μΩ·cm, respectively, which were in good agreement with published data of 11.5 and 107 μΩ·cm.[5)] The wettability was measured by the wetting angle of solders on Cu and Ni substrates. Solder alloys (0.3 g in mass) were put on both substrates. The 0.5 mm thick substrate was polished with 1 μm diamond paste and cleaned in aceton and ethanol solution. Soldering was performed in a convection reflow furnace longer than 60 s. The peak temperature was 330°C. The wetting angle was calculated from a cross section view of the joint specimen.[6)]

*Corresponding author: E-mail: hmlee@kaist.ac.kr

3. Results

3.1 Sn–Sb system

The Sn–5Sb system is an alloy with a high melting point that has been developed to replace the widely used Sn–37Pb solder.[4] According to the calculated phase diagram of Sn–Sb shown in Fig. 1,[7] the melting temperature of Sn–5Sb is 240°C and it is slightly low for high temperature applications. Hence, an additional Sn–10Sb alloy with a higher amount of Sb was chosen as another candidate together with Sn–5Sb.

Figure 2 shows SEM images by secondary electron (SE) mode of as-cast Sn–5Sb and Sn–10Sb alloys. While the β-Sn matrix was observed without a secondary phase in Sn–5Sb, the distribution of secondary particles was observed in Sn–10Sb. Figure 3 shows XRD patterns of as-cast Sn–5Sb and Sn–10Sb alloys. Although the β-Sn matrix was observed alone without any secondary phase through SEM observation of Sn–5Sb, the existence of the β-SbSn phase was detected together with β-Sn in both alloys. The secondary phase was identified as β-SbSn. The distribution of β-SbSn particles in the β-Sn matrix may result in improvement of mechanical properties and the Vickers hardness increased from 20.04 to 29.5 Hv with an increased Sb content from 5 to 10 mass%. Although the resistivity of Sn–Sb increased with Sb, it was similar to that of 95Pb–5Sn. It has been reported that the wettability of Sn–Sb was improved with Sb,[8,9] however, it decreased in this work. The basic properties of Sn–Sb alloys and other solder candidates are listed in Table 1. The electrical resistivity of Au–20Sn is from Tummala *et al.*[10]

3.2 Bi–Ag system

The melting point of Bi is 271°C and it satisfies the temperature requirement for step soldering while the resistivity of Bi is 107 μΩ·cm and it is not suitable for high performance devices. As the conductivity of Ag is better, the addition of Ag to Bi is supposed to reduce resistivity. The calculated phase diagram of the binary Bi–Ag system is shown in Fig. 4.[11,12] The Bi–2.5Ag alloy can be a good candidate because this composition is eutectic. The Bi–5Ag solder that contains more Ag was also selected to lower the resistivity.

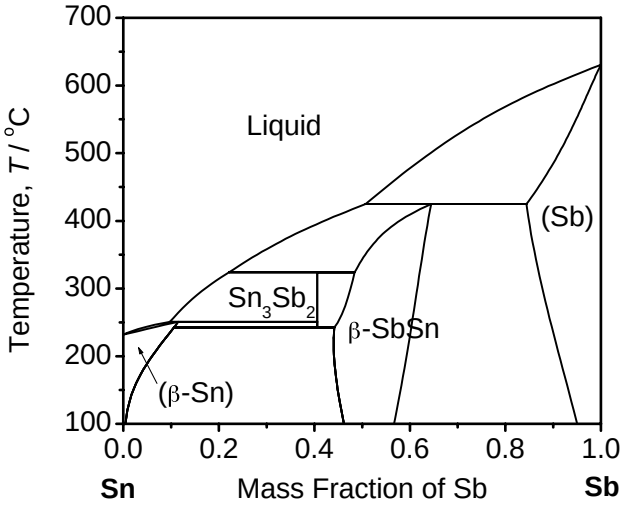

Fig. 1 Calculated phase diagram of the binary Sn–Sb system.[7]

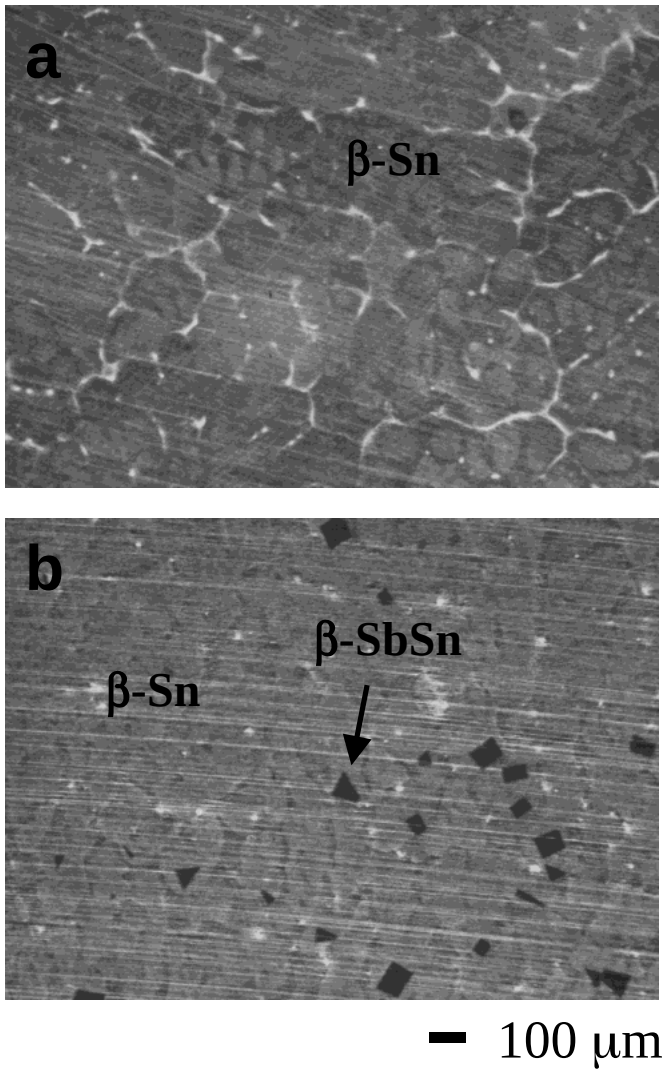

Fig. 2 SEM micrographs of as-cast (a) Sn–5Sb and (b) Sn–10Sb. SE mode used.

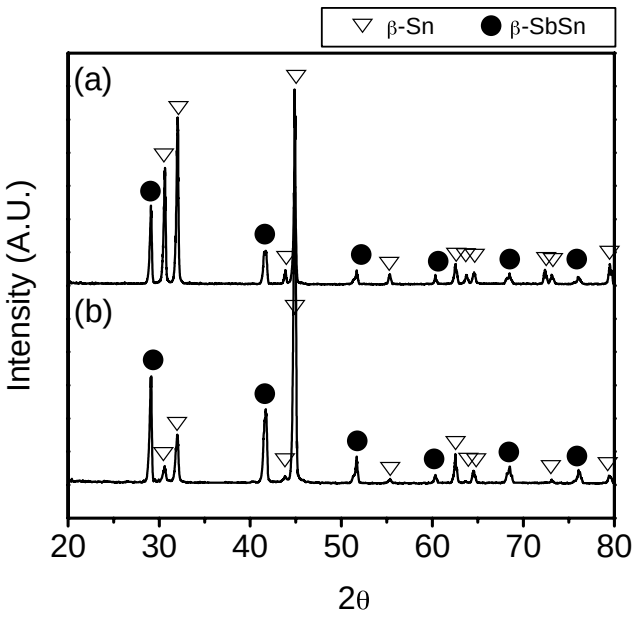

Fig. 3 XRD patterns of (a) Sn–5Sb and (b) Sn–10Sb.

Table 1 Properties of solder candidates compared with Pb–5Sn solder

Solder (mass%)	Vickers hardness (Hv)	Electrical resistivity (μΩ·cm)	Wetting angle (degree)	
			Cu substrate	Ni substrate
Pb–5Sn	8.9 (±0.17)	17.47 (±0.66)	21.37	20.21
Sn–5Sb	20.0 (±0.97)	15.87 (±2.20)	13	14
Sn–10Sb	29.5 (±3.13)	22.00 (±0.53)	46	28
Bi–2.5Ag	15.0 (±0.99)	110.30 (±0.83)	79	91
Bi–5Ag	15.2 (±2.5)	123.60 (±8.43)	62	118
Au–20Sn	200.8 (±13.78)	16*	33.05	64.56
Au–20Sn–5Sb	200.2 (±9.11)	33.29 (±1.10)	55.85	69.39

*Electrical resistivity of Au–20Sn is from Ref. 10).

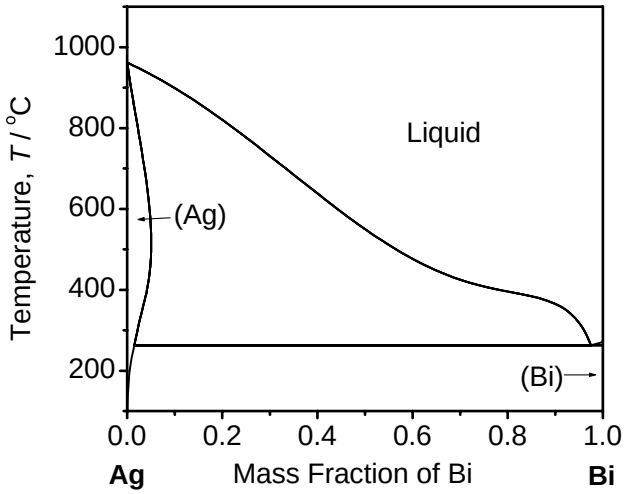

Fig. 4 Calculated phase diagram of the binary Ag–Bi system.[11,12]

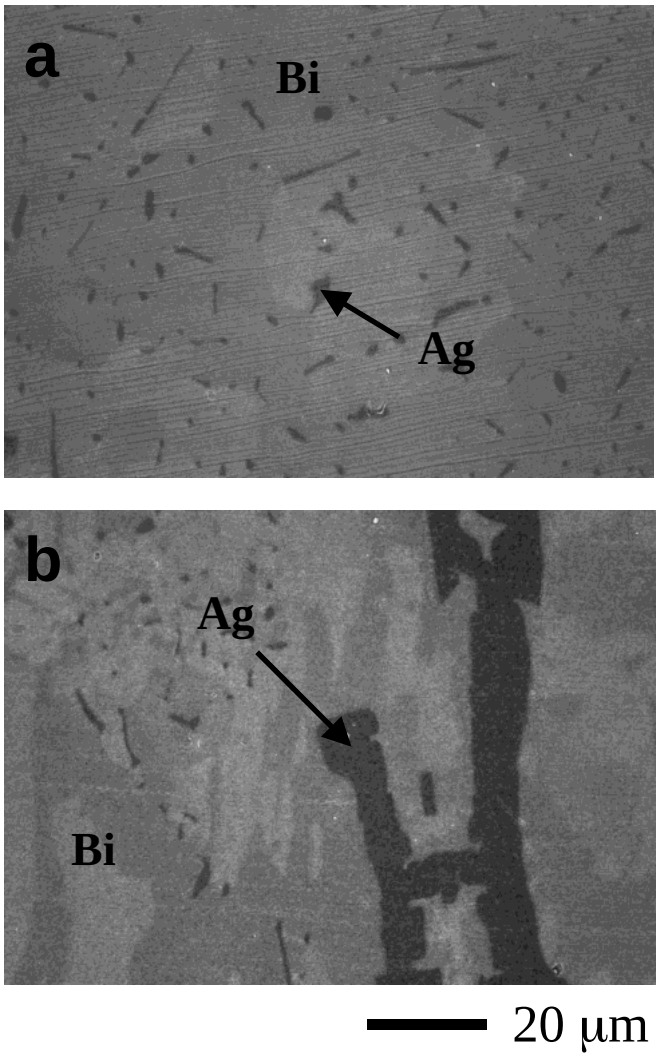

Fig. 5 SEM micrographs of as-cast (a) eutectic Bi–2.5Ag and (b) off-eutectic Bi–5Ag. BS mode used.

Figure 5 shows SEM images by back-scattered (BS) mode of as-cast eutectic Bi–2.5Ag and off-eutectic Bi–5Ag. In Fig. 5(a), the distribution of Ag particles in the Bi matrix is observed clearly, and the primary Ag phase of the capital letter 'H' shape is observed in Fig. 5(b). The XRD patterns of Bi–2.5Ag and Bi–5Ag are shown in Fig. 6. The resistivity of the Bi–Ag alloy was originally supposed to decrease with Ag content, however, the addition of Ag to Bi did not reduce the resistivity of the Bi–Ag solder alloy probably due to the heterogeneous microstructure. This must have exerted a pronounced effect in impeding the electron motion, thereby increasing resistivity.[13] The Bi–Ag alloys showed poor wettability on both Cu and Ni substrates. The hardness values of Bi–2.5Ag and Bi–5Ag alloys were similar to that of Pb–5Sn, but the Bi–Ag alloys showed weak and brittle behavior during handling of the specimen.

3.3 Au–Sn–Sb system

The Au–Sn solder has been used in the flip chip[14] because the melting point of Au–20Sn, 280°C, satisfies the temperature requirement. Due to the high cost of Au, the Au content needs to be reduced. It has been reported that alloying of Sb to Au–20Sn does not alter the melting temperature significantly.[15] In this regard, the Au–Sn–Sb system was chosen in this work and the phase diagram was calculated and shown in Fig. 7.[16] The differential scanning calorimeter (DSC) analysis was performed especially for Au–20Sn–5Sb to observe the melting behavior. Both alloys of Au–20Sn and Au–20Sn–5Sb were tested here.

Figure 8 shows the BS-SEM images of the as-cast Au–20Sn–5Sb alloy. The typical eutectic lamellar structure was observed in the matrix. The elongated gray particles were identified as AuSn. A line compound of the $Au(Sb, Sn)_2$ phase[15,16] exists according to phase equilibria, which implies that the Sb site in $Au(Sb, Sn)_2$ is substituted by Sn atoms. The blocky dark gray particles were determined as $AuSb_2$ and

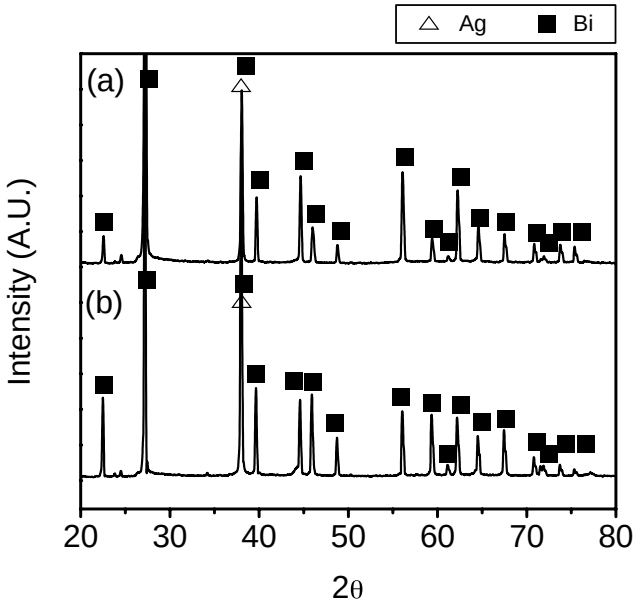

Fig. 6 XRD patterns of (a) Bi–2.5Ag and (b) Bi–5Ag.

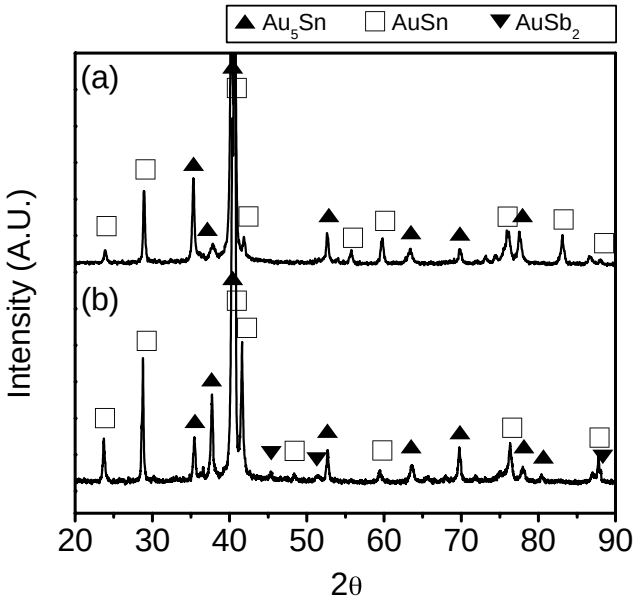

Fig. 9 XRD patterns of (a) Au–20Sn and (b) Au–20Sn–5Sb.

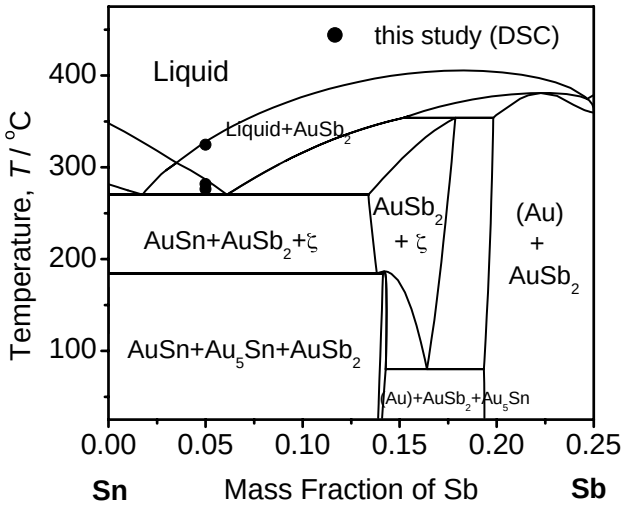

Fig. 7 Isoplethal phase diagram calculated along a constant amount of 75 mass%Au in the ternary Au–Sb–Sn system.[16] Symbols represent DSC data in this study.

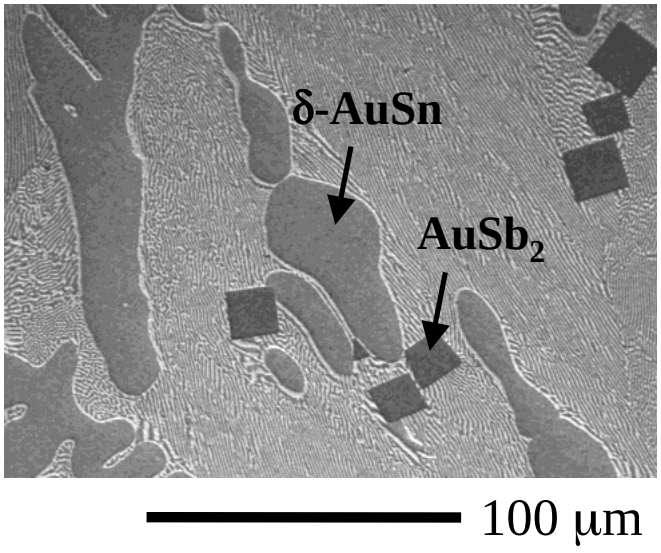

Fig. 8 SEM micrographs of as-cast Au–20Sn–5Sb. BS mode used.

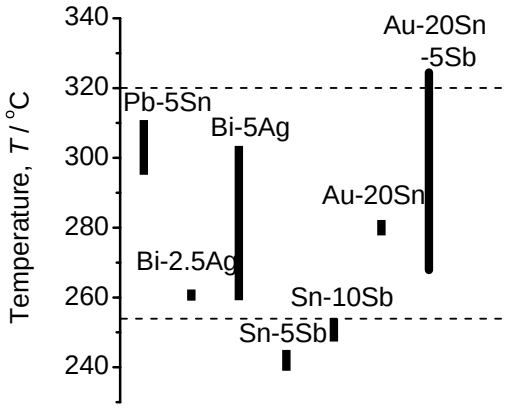

Fig. 10 Calculated melting temperatures of solders. The dotted line shows the melting range required for step soldering in MCM when the Sn–3.5Ag solder is used in the next level packaging.

the Sn content in this phase was measured at about 15 at%. Figure 9 shows XRD patterns of Au–20Sn and Au–20Sn–5Sb. The Vickers hardness did not change much with an addition of 5Sb. The resistivity and the wetting angle increased with alloying of 5Sb.

4. Discussion

The calculated melting temperatures of selected solders and the required melting temperature range for step soldering are presented in Fig. 10. As the polymer with a glass transition temperature of around 350°C[3] is used as dielectric materials of substrate, the upper limit of the melting temperature of high temperature solders is 320°C in considering that the reflow temperature is about 30°C higher than the melting temperature of solders. If the Sn–37Pb solder is used in the next level packaging, the lower melting temperature limit is 215°C which is 30°C higher than the melting temperature of Sn–37Pb, 183°C. When the Sn–3.5Ag solder is used for the next level, the lower melting temperature limit is 255°C because the melting point of Sn–3.5Ag is 221°C. Assuming

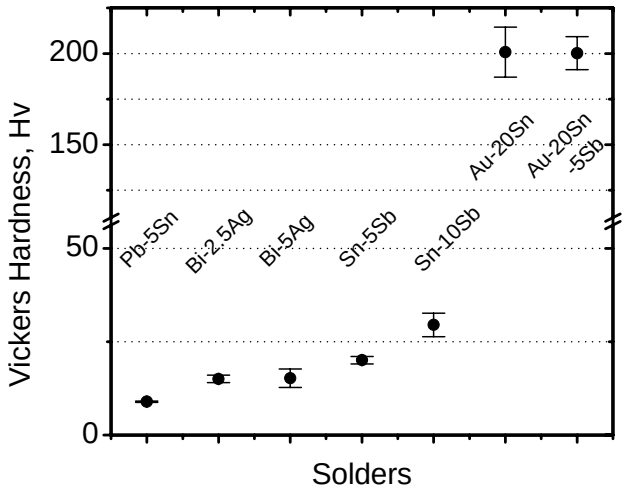

Fig. 11 Vickers hardness of solders.

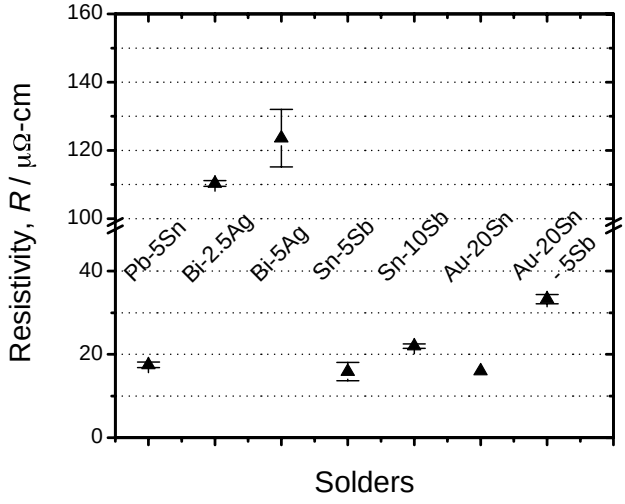

Fig. 12 Resistivity of solders. The data of Au–20Sn are from Ref. 10).

that the Sn–3.5Ag solder is used in the next level packaging, the required melting temperature for step soldering is between 255 to 320°C. According to Fig. 10, Sn–5Sb and Sn–10Sb are not suitable for high temperatures when Sn–3.5Ag is used in the subsequent packaging. Other solders are satisfactory in terms of the melting temperature. The liquidus temperature of Au–20Sn–5Sb is higher than 320°C and the melting range is so wide that modification of composition may be necessary.

Vickers hardness values of various solders are shown in Fig. 11. All of them are larger than that of Pb–5Sn, 8.9 Hv. The hardness of Au–20Sn and Au–20Sn–5Sb is, especially, 20 times as large as that of Pb–5Sn, and the addition of 5Sb did not change the hardness of Au–20Sn. Kloeser *et al.*[14] tested the Au–20Sn bump electroplated on Pd/Ag metallization and found that no electrical failures occurred in the chips with underfill after 6500 thermal cycles. The hard solders of Au–20Sn and Au–20Sn–5Sb appear to sustain high enough stress with proper underfill. Although the hardness of Bi–2.5Ag and Bi–5Ag is similar to that of Pb–5Sn, the Bi–Ag alloy showed brittleness during experiments. This alloy looks unsuitable for solder alloy because of weak and brittle behavior.

The resistivitiy of solder candidates is shown in Fig. 12.

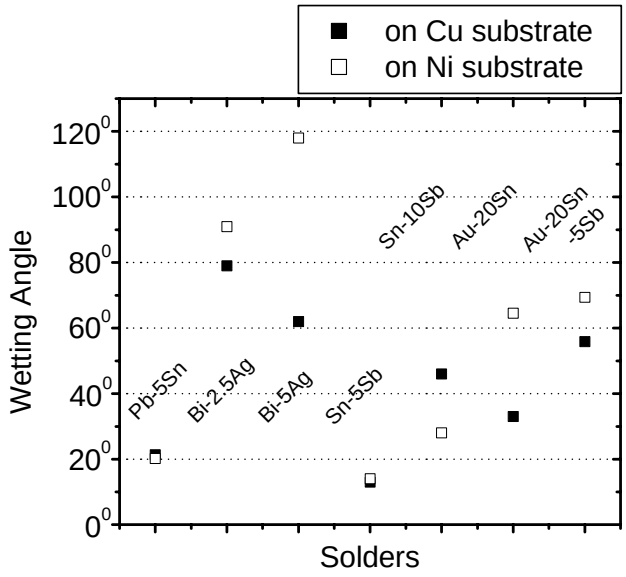

Fig. 13 Wetting angle of solder candidates measured on Cu and Ni substrates.

Except for Bi–2.5Ag and Bi–5Ag, the resistivity is similar to that of Pb–5Sn. The resistivity of Bi–2.5Ag and Bi–5Ag is so large that Bi–Ag systems may be unsuitable for high performance devices. The wetting angles measured on Cu and Ni substrates are shown in Fig. 13. The Bi–2.5Ag and Bi–5Ag alloys showed poor wettability on both Cu and Ni substrates, and the Sn–5Sb and Sn–10Sb alloys exhibited good wettability that is compatible with that of Pb–5Sn. It is, however, notable that the good wettability of Sn–Sb alloys may have come from the high reflow temperature, 80°C higher than the melting temperature of Sn–Sb alloys. The Au–20Sn and Au–20Sn–5Sb alloys showed high wetting angles, which necessitates the development of wettable layers such as Pd/Ag[14] for under bump metallurgy (UBM) of the Au–Sn–Sb solder system.

5. Summary

Three kinds of Sn–Sb, Bi–Ag and Au–Sn–Sb alloys were selected to replace the Pb–5Sn solder for step soldering used in MCM and they were investigated in terms of melting behavior, electrical resistivity, wetting angle and hardness. The Bi–Ag solders exhibited poor properties in all the tests. The Sn–Sb solders showed desirable properties but it is likely that the next level packaging process may affect the Sn–Sb solder. The Au–Sn and Au–Sn–Sb solders showed a high potential as Pb-free high temperature solders only with further modification of compositions for improvement of melting behavior and the development of UBM to enhance wetting.

Acknowledgments

This study has been supported by CEPM (Center for Electronic Packaging Materials) of the KOSEF (Korea Science and Engineering Foundation).

REFERENCES

1) G. L. Ginsberg and D. P. Schnorr: *Multichip Modules and Related Technologies*, (McGraw-Hill, New York, 1994) pp. 19–22.
2) M. McCormack and S. Jin: JOM **45** (1993) 36–40.
3) G. L. Ginsberg and D. P. Schnorr: *Multichip Modules and Related Technologies*, (McGraw-Hill, New York, 1994) pp. 135–138.
4) S. K. Kang, J. Horkans, P. C. Andricacos, R. A. Carruthers, J. Cotte, M. Datta, P. Gruber, J. M. E. Harper, K. Kwietniak, C. Sambucetti, L. Shi, G. Brouillette and D. Danovitch: 49th Electronic Components and Technology Conference, (San Diego, 1999) 283–288.
5) *CRC Handbook of Chemistry and Physics*, 79th Ed., (CRC Press, Cleveland, 1998-1999) pp. 12–45.
6) Z. Mei and J. W. Morris, Jr.: J. Electron. Mater. **21** (1992) 599–607.
7) B. Jonsson and J. Agren: Mater. Sci. Techn. **2** (1986) 913–916.
8) J. W. Jang, P. G. Kim and K. N. Tu: J. Mater. Res. **14** (1999) 3895–3900.
9) B.-J. Lee and H. M. Lee: *Design and Reliability of Solders and Solder Interconnections*, (TMS, Warrendale, 1997) pp. 129–136.
10) R. R. Tummala, E. J. Rymasezewski and A. G. Klopfenstein: *Microelectronics Packaging Handbook*, (Chapman and Hall, New York, 1997) pp. I-86.
11) B. Zimmermann: *Ph. D. Thesis*, (University of Stuttgart, Stuttgart, 1976).
12) U. R. Kattner and W. J. Boettinger: J. Electron. Mater. **23** (1994) 603–610.
13) R. A. Flinn and P. K. Trojan: *Engineering Materials and Their Applications*, 4th ed., (John Wiley and Sons, New York, 1990) pp. S-113.
14) J. Kloeser, E. Zakel, F. Bechtold and H. Reichl: IEEE CPMT **19A** (1996) 24–33.
15) A. Prince, G. V. Raynor and D. S. Evans: *Phase Diagrams of Ternary Gold Alloys*, (Institute of Metals, London, 1990) pp. 411–413.
16) J. H. Kim, S. W. Jeong and H. M. Lee: J. Electron. Mater. **31** (2002) 557–563.